

# Unified Membrane Fouling Index for Low Pressure Membrane Filtration of Natural Waters: Principles and Methodology

HAIQIU HUANG, THAYER A. YOUNG, AND JOSEPH G. JACANGELO\*

Center for Water and Health, Johns Hopkins University, 615 North Wolfe Street, Baltimore, Maryland 21205

Received May 3, 2007. Revised manuscript received October 31, 2007. Accepted November 6, 2007.

Membrane filtration is considered an important technology that can contribute to the sustainability of water supplies. However, its continued development necessitates the establishment of proper techniques for the assessment of membrane fouling. Unified Membrane Fouling Index (UMFI) was developed in this study in order to quantify and assess the fouling of low-pressure membranes (LPM) observed at various scales of water treatment. The foundation of UMFI is a revised Hermia model applied to both constant pressure and constant flux filtration. The adoption of UMFI makes it possible to simplify and standardize the bench-scale testing of membrane fouling potential by directly using the commercial LPM of interest. This approach can overcome a major challenge to fouling assessment, i.e., the membrane-specificity of fouling potential, which has not been wholly addressed by existing fouling indices. The fundamentals of UMFI are presented in this paper, together with the methodology for bench-scale testing. The application of UMFI to the assessment of the fouling of a LPM by a natural surface water is also discussed. Good agreement between bench-scale UMFI and pilot-scale UMFI was found, suggesting the validity of this new scientific concept for environmental applications.

## Introduction

Low-pressure membrane (LPM) filtration, which includes microfiltration (MF) and ultrafiltration (UF), is one of the most important technology advances that has occurred in the field of water treatment in the past two decades. The application of LPM filtration is, however, still hindered by the problem of membrane fouling. Membrane fouling, or the loss of membrane permeability due to the accumulation of aquatic contaminants on or within the membrane, is ubiquitously observed with LPM used at different scales of water treatment. Recent studies have found that a certain fraction of natural organic matter (NOM) (1, 2) or wastewater organic matter (3) probably contributes most to this phenomenon, and the magnitude of the fouling caused by NOM, especially the irreversible part, is often specific to each membrane and feedwater combination (4). Because of this specificity, the fouling potential of a particular feedwater is difficult to quantify based on a single membrane test. Most membrane fouling indices (MFI) rely on the use of surrogate

membranes, rather than those employed in actual water treatment. The specificity of membrane fouling makes it difficult to use these indices to predict the extent of fouling at greater scales. Therefore, the primary goal of this work was to develop a unified membrane fouling index (UMFI) that can quantify the fouling potential of an individual membrane and water combination by directly testing the fouling of commercially available membranes. The index was mathematically derived in such a way that it can be directly applied to LPM filtration operated at different scales or modes (constant pressure versus constant flux). The intent of universality was to provide the capability to scale up or cross compare the specific fouling results encountered in different LPM systems. The combination of specificity and universality is the most important feature of UMFI.

This study was undertaken with three specific objectives: (1) to elucidate the mathematical development of UMFI and its relationship to other MFIs, (2) to introduce an experimental method that can be used to determine UMFI, and (3) to determine, for the same membrane and water combination, whether the UMFI obtained at bench scale can be used to predict membrane fouling observed at a larger scale.

## Theoretical Basics

**Hermia's Model and Traditional Fouling Indices.** A blocking model based for four simplified fouling modes has been used in evaluating the fouling of membranes by various types of water matrices with complex compositions since it was first established by Hermia (5). The characteristic form of the Hermia model is:

$$\frac{d^2t}{dV^2} = k \left( \frac{dt}{dV} \right)^n \quad (1)$$

where  $t$  [second] and  $V$  [m<sup>3</sup>] are the filtration time and cumulative permeate volume, respectively, and  $k$  and  $n$  are two model parameters with varying values or dimensions. In them,  $n$  is a dimensionless number that is related to the fouling mechanism as introduced later;  $t$  and  $V$  are obtained from constant pressure filtration experiments. Schematic diagrams of the four fouling modes proposed by Hermia are presented in Figure 1.

A feature of the model is that it clearly defines several idealized but relevant fouling modes (or boundary conditions for nonideal situations) that can be described using very simple mathematical expressions summarized by eq 1. The deviation of experimental fouling data from these relationships set by eq 1 is attributed to the complicated nature of membrane filtration systems and the coincidence of different modes of fouling. Another feature of the model is that it does not explicitly rely on any information with regard to foulant rejection. For constant pressure filtration, experimental data on cumulative permeate volume and filtration time are sufficient for implementing the model for the purpose of data evaluation. Even though it is unable to provide a detailed picture of membrane fouling in the absence of rigorous consideration of the temporal variation in foulant rejection, the model serves as a useful tool to assess experimental data and point out the directions needed for further mechanistic studies. The combination of the model with other experimental techniques, such as in situ characterization of fouling layers, may be used to explore the fouling mechanism relevant to membrane filtration of natural waters.

Several membrane fouling indices (MFIs) have been proposed based on the Hermia model by assuming that cake layer formation is the dominant mode of membrane fouling

\* Corresponding author e-mail: joe.g.jacangelo@us.mwhglobal.com.

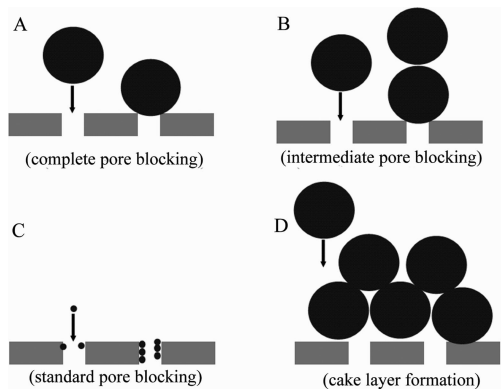


**FIGURE 1. Schematic diagram of the four modes of membrane fouling proposed by Hermia.**

encountered in the application of membrane filtration to water treatment. Those MFIs include the silt density index (SDI, ASTM D4189-95), MFI with MF membrane (6), MFI with UF membrane (7–9), MFI with NF membrane (10), and other (11). As measurements of the fouling tendency, SDI and MFIs involve a constant-pressure membrane filtration test using a reference flat-sheet membrane. The fouling indices are then calculated from the experimentally determined relationship between filtration time and cumulative permeate volume. For cake layer formation,  $n = 0$  in eq 1, and integration of eq 1 yields

$$\frac{dt}{dV} = (\text{MFIs}) V \quad (2)$$

Here parameter  $k$  in eq 1 is substituted by MFIs. Equation 2 shows that the greater the MFIs, the smaller the  $dV/dt$ , indicating that less water passes through the fouled membrane per unit time at a given cumulative permeate volume. Therefore, these MFIs provide simple evaluation of the fouling potential of a raw water to be treated.

An important limitation of the original model developed by Hermia is that it was derived solely for constant-pressure systems. Therefore,  $(dt/dV)$  is used as the basic parameter to evaluate the rate of fouling. In contrast, most full-scale LPM filtration systems are designed and operated in the constant flux mode, i.e., the permeate flow rate remains constant throughout the filtration process. In this case,  $(dt/dV)$  on the left-hand side (LHS) of eq 2 is a constant equivalent to the inverse of flow rate, while the cumulative permeate volume term on the right-hand side (RHS) increases as filtration time increases. Thus, the MFIs expressed by eq 2 cannot be a constant parameter. To apply the model to constant flux filtration, the basic expressions of the model warrant revision by integrating a constant flow operational condition.

#### Revision of Hermia Model for Constant Flux Filtration.

**Complete Pore Blocking.** Complete pore blocking occurs when all particles reaching the membrane only participate in the “sealing” of membrane pores as illustrated in Figure 1A. This idealized condition assumes that none of the particles are situated on top of other particles (i.e., no cake layer formation) or on the solid area of the membrane surface between pores. Therefore, the area of membrane surfaces with open pores ( $A_t$ ,  $\text{m}^2$ ) decreases linearly with the number of particles reaching the membrane or with the projected area of the particles on the membrane surface ( $A_p$ ,  $\text{m}^2$ ). For a given particle suspension, the latter can be expressed as

$$A_p = \sigma m_f \quad (3)$$

where  $m_f$  [kg] is the mass of particles that attach to membrane surfaces and cause fouling, and  $\sigma$  [ $\text{m}^2/\text{kg}$ ] is the projected area of these particles on the membrane

surface normalized to a unit mass of particles, a characteristic of the suspension.

For a monodispersed suspension,

$$\sigma = \frac{1.5}{\rho d \psi} \quad (4)$$

where  $\rho$  [ $\text{kg}/\text{m}^3$ ] is the particle density,  $d$  [m] is the diameter of particles, and  $\psi$  [dimensionless] is the shape factor ( $0 < \psi \leq 1$ ). A  $\psi$  value of unity corresponds to spheres.

Further,  $A_t$  can be expressed as

$$A_t = A_0 - A_p = A_0 - \sigma m_f \quad (5)$$

where  $A_0$  is the initial pore area of the membrane. Hence,

$$\frac{dA_t}{dm_f} = -\sigma \quad (6)$$

The transmembrane pressure required to drive the permeate through the membrane ( $P$ , Pa) is related to the permeate flowrate ( $Q$ ,  $\text{m}^3/\text{second}$ ) and  $A_t$  following Darcy’s law

$$Q = \frac{PA_t}{\mu R_m} \text{ or } P = \frac{Q\mu R_m}{A_t} \quad (7)$$

where  $R_m$  [ $\text{m}^{-1}$ ] is the hydraulic resistance of the membrane. For constant flow membrane filtration,  $Q$  remains constant during filtration and  $P$  increases as a result of membrane fouling. At any time during the filtration,  $PA_t = P_0A_0 = \mu R_m Q$  as shown in eq 7, where  $P_0$  and  $A_0$  are the initial transmembrane pressure and the pore area of the membrane surface, respectively. The characteristic rate of fouling in constant flow membrane filtration is  $dP/dm_f$ , which describes the rate at which the transmembrane pressure would increase per unit mass of aquatic materials being filtered. It is related to the decrease of open membrane pore area as follows (note according to eq 7,  $PA_t = P_0A_0 = \text{constant}$  when  $Q = \text{constant}$ ):

$$\frac{dP}{dm_f} = \frac{d}{dm_f} \left( \frac{\mu R_m Q}{A_t} \right) = - \left( \frac{P^2}{P_0 A_0} \right) \frac{dA_t}{dm_f} \quad (8)$$

By inserting eq 6 into eq 8, we have:

$$\frac{dP}{dm_f} = \left( \frac{\sigma}{P_0 A_0} \right) P^2 \quad (9)$$

Equation 9 can be further simplified by introducing two normalized parameters,  $P'$  [dimensionless] and  $m'_f$  [ $\text{kg}/\text{m}^2$ ]:

$$\frac{dP'}{dm'_f} = \sigma P'^2 \quad (10)$$

where  $P'$  and  $m'_f$  are defined as follows:  $P' = P/P_0$  and  $m'_f = m_f/A_0$ .

**Intermediate Pore Blocking.** In the case of intermediate pore blocking (Figure 1B), each particle reaching the membrane may not only block membrane pores as in the case of complete pore blocking, but also attach to other particles on the membrane surface. With this concept, existing particles on the membrane surface serve as competitors with membrane pores for approaching particles and reduce the actual number of particles that can block the pores. Therefore, an analysis of pore blocking probability into the previous discussion of complete pore blocking is necessary. The probability for a particle to block membrane pores at any time is equivalent to the ratio of the remaining open pore area,  $A_t$ , to the initial total open pore area,  $A_0$ . Hence, the decrease of the open membrane pore area as a unit mass of particles being retained is just  $\sigma$  multiplied by the unit mass of particles blocking membrane pores:

$$\Delta A_t = -\sigma \Delta m_f \left( \frac{A_t}{A_0} \right) \quad (11)$$

where  $\sigma \Delta m_f$  is the total area covered by unit mass of particles. This value multiplied by the probability for pore blocking gives the loss of membrane pore area caused by unit mass of particles. Equation 11 can be written in a differential form:

$$\Delta A_t = -\sigma \Delta m_f \left( \frac{A_t}{A_0} \right) \quad (12)$$

Solving this equation with a boundary condition of  $A_t = A_0$  at  $V = 0$ , we have

$$\frac{dA_t}{dm_f} = -\sigma \left( \frac{A_t}{A_0} \right) \quad (13)$$

By incorporating eq 13 into eq 8 and also recognizing that

$$A_t = A_0 \exp \left( -\frac{\sigma m_f}{A_0} \right) \quad (14)$$

the fouling rate for intermediate pore blocking is obtained:

$$\frac{P_0}{P} = \frac{A_t}{A_0} = \exp \left( -\frac{\sigma m_f}{A_0} \right) \quad (15)$$

Similar to eq 9, eq 15 can be converted to a normalized form:

$$\frac{dP}{dm_f} = \left( \frac{\sigma}{A_0} \right) P \quad (16)$$

**Standard Pore Blocking/Pore Constriction.** As shown in Figure 1C, standard pore blocking results from the constriction of membrane pores by small particles attached internally to pore walls. Assuming that the membrane consists of  $N$  uniform cylindrical pores with a radius of  $r_0$  and a length of  $L$  and that the radius of the pores decreases at the same rate as particles attach to their walls, the following mass balance relationship is established to determine the effective pore radius after fouling ( $r$ ):

$$N\pi(r_0^2 - r^2)L = \frac{m_f}{\rho} \quad (17)$$

With the aforementioned assumptions, the transmembrane pressure of the membrane is inversely proportional to the radius of the pores following Poiseuille's equation (12):

$$P = \frac{8\mu L Q}{N\pi} \times \frac{1}{r^4} \quad (18)$$

Consequently, the normalized transmembrane pressure is simply:

$$P' = \frac{P}{P_0} = \frac{r_0^4}{r^4} \quad (19)$$

Combination of eqs 17 and 19 yields

$$\frac{dP'}{dm_f} = \left( \frac{2}{L\rho} \right) P'^{3/2} \quad (20)$$

**Cake Layer Formation.** Unlike pore blocking, the cake filtration type of fouling does not involve any changes to the pore structure of membranes. Instead, the increase of hydraulic resistance encountered during membrane filtration is caused by the formation of a cake layer outside the external membrane surface (Figure 1D). The cake layer resistance,  $R_c$  [ $m^{-1}$ ], is expressed as

$$R_c = \hat{R}_c \frac{m_f}{A_0} \quad (21)$$

**TABLE 1. Linear Expressions of UMFI for LPM Filtration Based on the Revised Hermia Model**

fouling mechanism	$n$	$k_v$ or UMFI	linear expression
cake formation	0	$C_f \hat{R}_c / R_m$	$1/j'_s = 1 + k_v V_s$
intermediate blocking	1	$C_f \sigma$	$\ln j'_s = -k_v V_s$
standard blocking	3/2	$2C_f / L\rho$	$j_s^{1/2} = 1 + k_v / 2V_s$
complete blocking	2	$C_f \sigma$	$J'_s = 1 - k_v V_s$

where  $\hat{R}_c$  [ $m/kg$ ] is the specific resistance of cake layer. Application of Darcy's law to cake layer filtration yields:

$$P = \frac{Qu(R_m + R_c)}{A_0} \text{ and } P_0 = \frac{QuR_m}{A_0} \quad (22)$$

Since  $R_m$  remains constant, the fouling rate is obtained by combining eqs 21 and 22:

$$\frac{dP}{dm_f} = \frac{Qu \hat{R}_c}{A_0^2} \quad (23)$$

or the normalized form:

$$\frac{dP'}{dm'_f} = \frac{\hat{R}_c}{R_m} \quad (24)$$

The RHS of eq 24 is independent of the transmembrane pressure if the cake is incompressible and  $\hat{R}_c$  remains constant, which may be considered independent of the pressure for low pressure membranes.

**Unified Model Expression.** Similar to the Hermia model for constant pressure filtration, eqs 10, 16, 20, and 24 can be combined into one simple expression as follows:

$$\frac{dP'}{dm'_f} = k_m P'^n \quad (25)$$

where  $k_m$  and  $n$  are two constants and vary for different modes of fouling. The  $n$  values are the same as those found in the constant pressure model. This consistency is reasonable as similar assumptions were used in the development of both models. The specific mass of foulants ( $m_f$ ) in eq 25 cannot be readily determined in filtration experiments. Therefore, it is necessary to assume that the retention of foulants by the membrane is a constant independent of increasing filtration time (or permeate throughput,  $V_s$  [ $m^{-1}$ ], since it is constant flux filtration); this assumption was latent in the development of the constant pressure model as well and is appropriate for most LPMs that work as surface filters in water treatment. For some LPMs functioning as deep filters, the retention of foulants is possibly time-dependent. Given the aforementioned assumption, eq 25 can be converted to

$$\frac{dP'}{dV_s} = k_v P'^n \quad (26)$$

where  $V_s$  [ $m^3/m^2$  or  $L/m^2$ ] is the unit permeate throughput defined as the cumulative volume of permeate per unit membrane surface area,  $k_v$  is a fouling parameter that equals  $k_m$  multiplied by foulant concentration in the feedwater,  $C_f$  [ $kg/m^3$ ] as listed in Table 1.

**Derivation of UMFI.** Equation 26 can be further converted into a function of normalized specific flux,  $J'_s$  [dimensionless], by introducing the definition of specific flux:  $J_s = J/P$  where  $J$  [ $m/s$ ] is the permeate flux and equals permeate flow rate per unit membrane surface area.

Then, the normalized specific flux is defined as:

$$J'_s = \frac{J_s}{J_{s0}} = \frac{1}{P'} \quad (27)$$

where  $J_{s0}$  is the  $J_s$  at time zero. Inserting eq 27 into eq 26 yields

$$-\frac{dJ'_s}{dV_s} = k_v J'_s{}^{2-n} \quad (28)$$

For constant pressure filtration, it is recognized that

$$\begin{aligned} \frac{dt}{dV} &= \frac{1}{(dV/dt)} = \frac{1}{JA_m} = \frac{1}{J_s PA_m} \\ \frac{d^2 t}{dV^2} &= \frac{d(1/J_s PA_m)}{dV} = -\frac{1}{J_s^2 PA_m} \frac{dJ_s}{dV} \end{aligned} \quad (29)$$

where  $P$  is a constant and  $A_m$  is the total membrane surface area. Inserting eq 29 into eq 1 gives

$$-\frac{dJ_s}{dV} = k(PA_m)^{1-n} J_s^{2-n} \quad (30)$$

Substitution of  $J_s$  and  $V$  in eq 30 with normalized terms will yield eq 28. Thus, eq 28 is valid for both constant flux and constant pressure filtrations. The use of normalized terms,  $J'_s$  and  $V_s$  also eliminates the impact of the total membrane surface area of the LPM system on the fouling parameter,  $k_v$ , a development that is important to the scale-up of UMFI.

If the value of  $n$  is superimposed for different modes of fouling, integration of eq 28 forms a set of linear equations as presented in Table 1. Of all four modes of fouling presented in this table, complete pore blocking is an idealized scenario for pore blocking that requires all foulants to accumulate solely on membrane pores. However, model simulation results (13) and experimental evidence (13–15) have shown that the deposition of foulants on LPM does not occur exclusively on membrane pores. Therefore, unlike previous studies (16), complete pore blocking is considered unimportant and excluded in the derivation of UMFI. The remaining three modes of fouling include cake layer formation and two modes of pore blocking (intermediate/standard pore blocking). Cake layer formation is the most universal type of membrane fouling in water treatment in that it does not rely on the existence of favorable membrane-contaminant attractions. Consequently, reversible fouling can occur even though a membrane is fabricated to be “non-sticky” to aquatic contaminants. By contrast, standard/intermediate pore blocking occurs in the presence of favorable membrane-contaminant attractions, and therefore, can be more resistant to hydrodynamic or mechanical forces applied during cleaning and more important to irreversible fouling.

Pore blocking and cake layer formation occur simultaneously in LPM fouling; their relative importance varies during long-term filtration. Different multistage models have been proposed in previous studies (16, 17). In those models, pore blocking is often considered to dominate the initial stage of fouling while cake layer formation becomes predominant in long-term operation. When this transition in fouling mechanisms occurs depends primarily on the manner in which the pore blocking efficiency is interpreted. Even for fouling caused by model substances with known physical and chemical properties (as compared to the unstable and diverse foulants in natural waters), the pore blocking efficiency was usually treated arbitrarily in those models as a fitting parameter that was difficult to be quantified independently. Another problem in multistage models is that the reversibility of fouling was usually ignored, which limits their application to water treatment practice. For a water

treatment plant, irreversible fouling (not total fouling) determines the long-term performance of LPM systems operated with frequent hydraulic and chemical cleanings. Irreversible fouling is the result of stable attachments of foulants on membrane surfaces that are resistant to hydraulic or chemical cleaning. As discussed previously, pore blocking caused by favorable foulant–membrane attractions is probably more important than cake layer formation in this case. Consequently, it is possible to approximate the long-term fouling with pore blocking models. The equations for standard and intermediate blocking (Table 1) can be expanded as Taylor series. The first order progressions of these equations are approximations of the equation for cake layer formation if  $k_v$  is small enough, which is probably true for natural waters as the concentration of major organic foulants in natural waters are often at a very low level (4, 18, 19). This makes it possible to define UMFI using a single equation. UMFI is thus defined based on the cake layer formation equation:

$$\frac{1}{J'_s} = 1 + (\text{UMFI}) V_s \quad (31)$$

The term has a unit of  $\text{m}^{-1}$ , or  $\text{m}^2/\text{L}$  if  $V_s$  has a unit of  $\text{L}/\text{m}^2$ . UMFI can be representative of total fouling, physically irreversible fouling, and chemically irreversible fouling if relevant  $J'_s$  and  $V_s$  are determined experimentally. Here, total fouling refers to membrane fouling observed before any hydraulic, pneumatic, or chemical cleaning; physically irreversible fouling refers to membrane fouling remaining after a physical (hydraulic and/or pneumatic) cleaning operation; chemically irreversible fouling is designated to the residual fouling observed after a chemical cleaning operation, such as caustic or chlorine treatment. It should be pointed out that UMFI defined in eq 31 provides a possible approach to assess LPM fouling potential (especially irreversible fouling) by directly employing the membrane of interest to large-scale applications, rather than any surrogates as proposed in previous studies (6, 9, 10, 20). The mathematical derivations presented here elucidate the origin of the relationship used in the calculation of UMFI, and are not complete interpretations of the fouling mechanisms. This linear relationship is simple and shows reasonable agreement with both bench-scale and pilot-scale experimental results as shown later. However, it is emphasized that data fitting is insufficient to validate a mechanistic model.

## Materials and Methods

**Natural Water.** Natural water was collected from White River, Indianapolis, IN. The properties of this water are presented in Table S1 of the Supporting Information (SI). For the purpose of bench-scale experiments, the water sample was prefiltered using  $1.2 \mu\text{m}$  glass fiber filters (Whatman, model GF/C) to remove coarse materials, including most bacteria and other microbiota. The same source of water was used in pilot tests without prefiltration.

### Low-Pressure Membrane and Membrane Filtration

**Units.** A commercially available hollow-fiber MF membrane was acquired from the manufacturer. This membrane was constructed of polyvinylidene fluoride (PVDF), having a nominal pore size of  $0.1 \mu\text{m}$ . For bench-scale experiments, 9 membrane fibers were potted into a direct flow mini module with an effective length of approximately  $0.25 \text{ m}$  and a membrane surface area of approximately  $0.0056 \text{ m}^2$ . All new modules were cleaned by filtering at least  $2 \text{ L}$  of ultrapure water prior to fouling experiment. For pilot-scale tests, full length modules were supplied by the manufacturers.

Both the bench-scale and the pilot-scale systems were operated in outside-in, constant flux mode. Bench-scale filtration was conducted at a permeate flux of  $80\text{--}110 \text{ L}/\text{m}^2\text{-hr}$  (lmh), and lasted for  $2\text{--}3 \text{ h}$ . Details of the bench-scale testing unit and

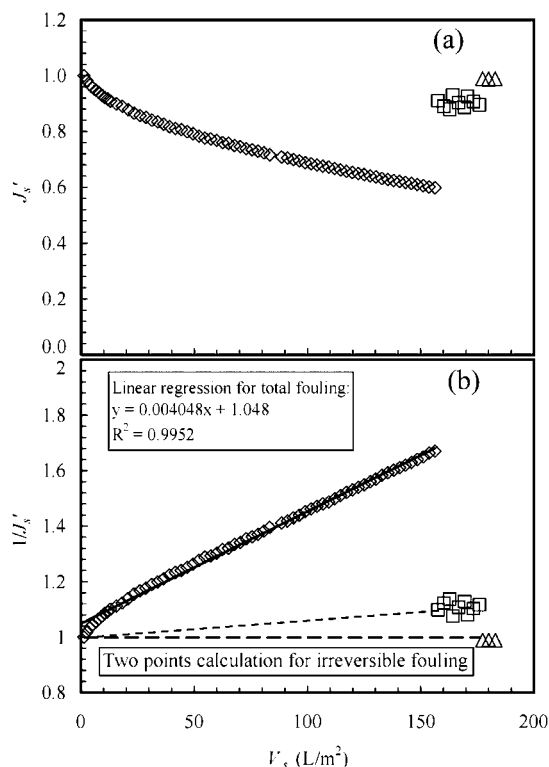


**FIGURE 2.**  $J_s$  (top graph) and  $1/J_s$  (bottom graph) as a function of specific permeate throughput,  $V_s$ . The experiment included a filtration cycle ( $\diamond$  a permeate flux of 82 l/mh, three permeate backwashes at 109, 163, and 218 l/mh with subsequent filtration cycles ( $\blacksquare$ ), and a chemical cleaning with a final filtration cycle ( $\triangle$ ). The short and long dashed lines and the solid line describe the calculation of UMFI values based on their slopes.

the operation protocol can be found elsewhere (4). The pilot-scale LPM testing unit was supplied by the manufacturer and operated in the field at similar fluxes. The operation of this pilot unit included filtration and intermittent permeate backwash with air scouring. Chemical cleaning of the fouled membrane was performed once per day at an equivalent permeate throughput of 1200–1400 L/m<sup>2</sup>.

## Results and Discussion

**Typical Fouling Results.** Typical fouling results from a bench-scale fouling experiment are presented separately as  $J_s$  versus  $V_s$  and  $1/J_s$  versus  $V_s$  in Figure 2a and b. As shown in the figure, UMFI for total fouling was calculated by unforced linear regression of the experimental data using eq 31. A nonlinear region was observed from the onset of filtration to a  $V_s$  of 10 L/m<sup>2</sup>. This region was not excluded from the regression for the simplicity of calculation; the resulting difference is negligible. The slope of the regression line ( $4.05 \times 10^{-5}$  m<sup>2</sup>/L) is the value of UMFI for total fouling. In comparison, UMFI for irreversible fouling was determined from the fouling curve using a “two-points” method. The short dashed line in Figure 2 connects the starting point of the fouling curve, (1, 0), and the first point for the filtration cycle after the first permeate backwash. The slope of this short dashed line ( $6.34 \times 10^{-4}$  m<sup>2</sup>/L) corresponds to a UMFI value for hydraulically irreversible fouling. Likewise, the long dashed line in Figure 2 connects the starting point of the fouling curve and the first point for the filtration cycle after the chemical cleaning; its slope (zero) represents the value of UMFI for chemical cleaning. Similar calculations were conducted based on pilot-scale fouling results. In general, either linear regression or two-points method was employed to calculate UMFI depending on the availability of experimental data.

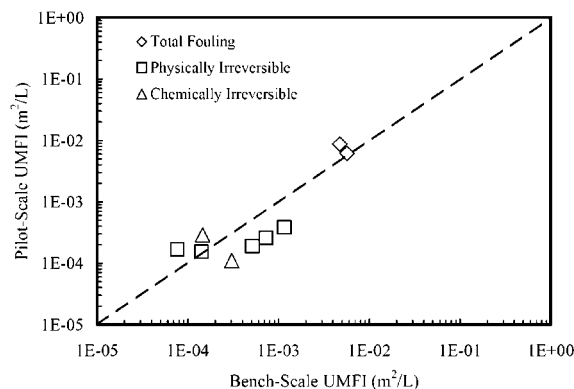


**FIGURE 3.** Correlation of bench-scale UMFI values with pilot-scale UMFI values for a low-pressure, hollow-fiber membrane fouled by White River, Indianapolis water. The dashed line with slope = 1 is shown for reference.

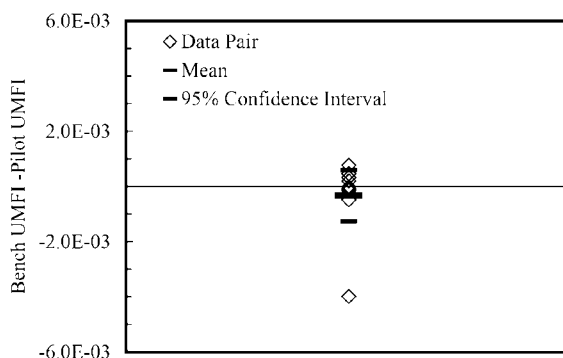


**FIGURE 4.** Matched pair analysis for the fouling of a low-pressure, hollow-fiber membrane by White River water at bench and pilot scale. The y-axis is expressed as the bench-scale UMFI minus the pilot-scale UMFI for total fouling, physically irreversible fouling, and chemically irreversible fouling, respectively. Nine pairs of data were used in the analysis.

The validity of the linear regression method in describing the total fouling was tested in this study using a data set published previously by the authors (4). It was found that this linear equation provides a good fit for the data set (Table S2, SI). The same method may be applied to irreversible fouling (Figure S1, SI).

**Matched Pair Analysis.** UMFI values calculated using the methods described previously were used to determine the correlation between bench-scale and pilot-scale UMFI for the fouling of the LPM by White River water. The results are presented in Figure 3. The dashed line in the figure represents a one-to-one match of the data pair. As shown in the figure, the two sets of data obtained at bench scale and pilot scale matched reasonably well, particularly for two pairs for total fouling.

A matched pair analysis was used to statistically assess the impact of system scale on UMFI values. All data pairs shown in Figure 3 were used in the analysis. For each pair, the difference between the bench UMFI and the pilot UMFI was calculated and plotted in Figure 4, together with the mean and the associated 95% confidence interval. As shown in Figure 4, the difference between the matched UMFI values for the bench and for the pilot systems were not statistically different from zero. These results show that the bench UMFI determined by the experimental system designed in this study provided a reasonable prediction for the fouling of the LPM pilot-scale unit.

**Practical Aspects of UMFI.** UMFI developed in this study makes it possible to quantitatively compare numerous membrane fouling results to each other and evaluate mem-

brane fouling potential under different conditions, regardless of membrane type, water source, and operation mode and scale. It also provides a predictive tool to assess the resistance of membranes to severe fouling at simple bench-scale setting prior to costly and labor-intensive pilot-scale or full-scale tests.

It is important to note that in the bench-scale studies, the raw water was prefiltered with a 1.2  $\mu\text{m}$  filter to preserve the samples under laboratory conditions. This did not appear to affect the consistency of the UMFI results between the bench scale and the pilot scale (Figure 2), probably due to the predominance of colloidal/dissolved aquatic materials in membrane fouling. Similar minor prefiltration effects were also observed by Howe et al. (21). It is also possible to eliminate potential prefiltration effects by directly using the raw water without prefiltering.

An important aspect when conducting predictive fouling tests is the representativeness of new membranes at bench scale to mature membranes employed in full-scale systems. The effect of long-term fouling on UMFI depends primarily on the extent of chemically irreversible fouling of the full-scale system, which is an indication of permanent changes to membrane properties that occur after long-term operation. If the irreversible fouling is insignificant, new membranes probably have properties similar to the mature ones, thereby being a reasonable reference for full-scale membranes. On the contrary, if the irreversible fouling is significant, old membranes harvested from the full-scale system (e.g., those collected during routine membrane replacements) can be adopted in bench-scale UMFI tests and compared to new fibers to determine the real differences. This problem may also be prevented by choosing membranes with minimum UMFI values for chemically irreversible fouling in the design phase of a full-scale system.

Filtration time is important to bench-scale UMFI test. The length of the test depends primarily on the time needed to achieve significant fouling and the availability of feedwater. In this study, bench-scale filtration proceeded until a  $J_s/J_{s0}$  value of 0.5 was reached or until 1 L of water was filtered. The resulting UMFI values can be assessed for the levels of fouling potential. As discussed previously (4), fouling potential of natural waters is not universal but membrane-specific. Cumulative probability distribution of UMFI values calculated based on a reported data set (4) is shown in Figure S2 in the SI. If cumulative probabilities of 0.33 and 0.67 are chosen as the threshold probabilities, the boundary UMFI values for low ( $p < 0.33$ ) and high ( $p > 0.67$ ) fouling potentials can be obtained as shown in the SI. These values may be used to evaluate the level of fouling potential once the UMFI values for a specific membrane and water combination are determined.

## Acknowledgments

We thank Dr. Charles R. O'Melia for his direction in the development of the revised Hermia model and Dr. NoHwa Lee for providing the water quality information. Dr. Gary Amy and Mr. Jim Lozier are acknowledged for their insightful comments in the development of the UMFI concept, and Dr. Chandra Mysore is acknowledged for leading the pilot study. Technical support from the membrane manufacturer and the assistance from Veolia USA and Indianapolis Water Works are highly appreciated. The funding for this study was partially provided by American Water Works Association Research Foundation and United States Environmental Protection Agency.

## Appendix A

$\Psi$  shape factor with values between 0 and 1, dimensionless

$\rho$	density of foulants, $\text{kg}/\text{m}^3$
$\sigma$	projected area of a unit mass of the particles on membrane, $\text{m}^2/\text{kg}$
$A_0$	total pore area of the membrane at the onsite of filtration, $\text{m}^2$
$A_m$	total geometric area of the membrane surface on the side exposed to the source water, $\text{m}^2$
$A_p$	total area of membrane surface pores blocked by foulant particles, $\text{m}^2$
$A_r$	total unblocked pore area on membrane surface, $\text{m}^2$
$C_f$	mass concentration of foulants in the source water, $\text{kg}/\text{m}^3$
$D$	diameter of foulant particles, m
$J$	permeate flux used in dead-end membrane filtration, $\text{m}/\text{s}$
$K$	fouling coefficient used in the Hermia model for constant pressure filtration
$k_p$	fouling coefficient used in the Hermia model for constant flux filtration
$k_v$	fouling coefficient used in the unified Hermia model for both constant flux and constant pressure filtrations
$L_m$	effective length of membrane pores, m
$m_f$	total mass of foulants, kg
$m'_f$	total mass of foulants per unit membrane surface area, $\text{kg}/\text{m}^2$
$N$	fouling parameter related to different modes of fouling defined in the Hermia model, dimensionless
$P$	transmembrane pressure for membrane filtration, Pa
$P'$	relative transmembrane pressure (transmembrane pressure during filtration normalized to that of clean membranes), dimensionless
$P_0$	transmembrane pressure for a clean membrane, Pa
$Q$	permeate flowrate through the entire membrane or module, $\text{m}^3/\text{s}$
$R_m$	hydraulic resistance of clean membranes without fouling, $\text{m}^{-1}$
$\hat{R}_c$	specific cake resistance, $\text{m}/\text{kg}$
$T$	filtration time, s
$V_s$	specific permeate throughput (cumulative volume of permeate per unit membrane surface area), $\text{m}^3/\text{m}^2$ or $\text{L}/\text{m}^2$

## Supporting Information Available

Properties of White River water,  $R^2$  values for linear regression calculation of UMFI for total fouling, linear regression calculation of UMFI for physically irreversible fouling, and cumulative distribution of UMFI values referred to in the paper. This material is available free of charge via the Internet at <http://pubs.acs.org>.

## Literature Cited

- Howe, K. J.; Clark, M. M. Fouling of microfiltration and ultrafiltration membranes by natural waters. *Environ. Sci. Technol.* **2002**, *36* (16), 3571–3576.
- Howe, K. J.; Marwah, A.; Chiu, K.-p.; Adham, S. S. Effect of coagulation on the size of MF and UF membrane foulants. *Environ. Sci. Technol.* **2006**, *40* (24), 7908–7913.
- Kimura, K.; Yamato, N.; Yamamura, H.; Watanabe, Y. Membrane fouling in pilot-scale membrane bioreactors (MBRs) treating municipal wastewater. *Environ. Sci. Technol.* **2005**, *39* (16), 6293–6299.
- Huang, H.; Lee, N.; Young, T. A.; Amy, G.; James, C. L.; Jacangelo, J. G. Natural organic matter fouling of low pressure, hollow fiber membranes: Effects of NOM source and hydrodynamic conditions. *Water Res.* **2007**, *41* (17), 3823–3832.

- (5) Hermia, J. Constant pressure blocking filtration laws - Application to power-law non-Newtonian fluids. *Trans. Inst. Chem. Eng.* **1982**, *60* (3), 183–187.
- (6) Schippers, J. C.; Verdouw, J. Modified Fouling Index, a Method of Determining the Fouling Characteristics of Water. *Desalination* **1980**, *32* (1–3), 137–148.
- (7) Roorda, J. H.; van der Graaf, J. H. J. M. New parameter for monitoring fouling during ultrafiltration of WWTP effluent. *Water Sci. Technol.* **2001**, *43* (10), 241–248.
- (8) Abogrean, E. M.; Boerlage, S. F. E.; Kennedy, M. D.; El-Azizi, I. M.; Galjaard, G.; Schippers, J. S. Water quality monitoring in membrane filtration systems. *Ann. N.Y. Acad. Sci.* **2003**, *984*, 85–96.
- (9) Boerlage, S. F. E.; Kennedy, M. D.; Dickson, M. R.; El-Hodali, D. E. Y.; Schippers, J. C. The modified fouling index using ultrafiltration membranes (MFI-UF): Characterisation, filtration mechanisms and proposed reference membrane. *J. Membr. Sci.* **2002**, *197* (1–2), 1–21.
- (10) Khirani, S.; Aim, R. B.; Manero, M.-H. Improving the measurement of the Modified Fouling Index using nanofiltration membranes. *Desalination* **2006**, *191* (1), 1–7.
- (11) Brauns, E.; Van Hoof, E.; Molenberghs, B.; Dotremont, C.; Doyen, W.; Leysen, R. A new method of measuring and presenting the membrane fouling potential. *Desalination* **2002**, *150* (1), 31–43.
- (12) Zeman, L. J.; Zydney, A. L. *Microfiltration and Ultrafiltration: Principles and Applications*; 1st ed.; Marcel Dekker, Inc.: New York, 1996.
- (13) Kosvintsev, S.; Cumming, I. W.; Holdich, R. G.; Lloyd, D.; Starov, V. M. Sieve mechanism of microfiltration separation. *Colloids Surf., A* **2004**, *230* (1–3), 167–182.
- (14) Li, H.; Fane, A. G.; Coster, H. G. L.; Vigneswaran, S. Direct observation of particle deposition on the membrane surface during crossflow microfiltration. *J. Membr. Sci.* **1998**, *149* (1), 83–97.
- (15) Hughes, D.; Tirlapur, U. K.; Field, R.; Cui, Z. F. In situ 3D characterization of membrane fouling by yeast suspensions using two-photon femtosecond near infrared non-linear optical imaging. *J. Membr. Sci.* **2006**, *280* (1–2), 124–133.
- (16) Bolton, G.; LaCasse, D.; Kuriyel, R. Combined models of membrane fouling: Development and application to microfiltration and ultrafiltration of biological fluids. *J. Membr. Sci.* **2006**, *277* (1–2), 75–84.
- (17) Kosvintsev, S.; Holdich, R. G.; Cumming, I. W.; Starov, V. M. Modelling of dead-end microfiltration with pore blocking and cake formation. *J. Membr. Sci.* **2002**, *208* (1–2), 181–192.
- (18) Huang, H. *Microfiltration Membrane Fouling in Water Treatment: Impact of Chemical Attachments*. Ph. D. Dissertation, Johns Hopkins University: Baltimore, MD, 2006.
- (19) Lee, N.; Amy, G.; Croue, J. P. Low-pressure membrane (MF/UF) fouling associated with allochthonous versus autochthonous natural organic matter. *Water Res.* **2006**, *40* (12), 2357–2368.
- (20) Boerlage, S. F. E.; Kennedy, M. D.; Aniye, M. P.; Abogrean, E.; Tarawneh, Z. S.; Schippers, J. C. The MFI-UF as a water quality test and monitor. *J. Membr. Sci.* **2003**, *211* (2), 271–289.
- (21) Howe, K. J.; Marwah, A.; Chiu, K.-p.; Adham, S. S. Effect of membrane configuration on bench-scale MF and UF fouling experiments. *Water Res.* **2007**, *41* (17), 3842–3849.

ES071043J